Received: 24 December 2018 | Accepted: 10 October 2019

DOI: 10.1002/jcb.29517

Journal of Cellular Biochemistry WILEY

RESEARCH ARTICLE

Downregulated microRNA-92a-3p inhibits apoptosis and promotes proliferation of pancreatic acinar cells in acute pancreatitis by enhancing KLF2 expression

Lan Ling[1] | Hai-Feng Wang[2] | Jing Li[2] | Yan Li[1] | Cheng-Dong Gu[1]

[1]Emergency Department, China-Japan Friendship Hospital, Beijing, China

[2]Nephropathy Department, China-Japan Friendship Hospital, Beijing, China

Correspondence
Cheng-Dong Gu, Emergency Department, China-Japan Friendship Hospital, No. 2, Yinghua East Street, Chaoyang, 10029 Beijing, China.
Email: gcdguchengdong@126.com

Abstract

Acute pancreatitis (AP) is known worldwide as one of the most common gastrointestinal diseases, prospectively leading to hospitalization coupled with increasing incidence. Several microRNAs (miRNAs) have been reported to be potential biomarkers for pancreatitis. In this study, we verified the hypothesis that miR-92a-3p is implicated in the development of AP by controlling the proliferation and apoptosis of pancreatic acinar cells (PACs) through the modulation of the Kruppel-like factor 2 (KLF2) and inflammatory factors in rats. Initially, we established a rat model of AP and extracted the pancreatic tissues. Then, the positive rate of KLF2 was measured using immunohistochemistry, and the expression of the related genes was determined by rReverse transcription quantitative polymerase chain reaction and Western blot analysis. The cell proliferation and apoptosis were measured by 5-ethynyl-2′-deoxyuridine assay and flow cytometry, and the contents of inflammatory factors were measured using enzyme-linked immunosorbent assay. AP rats presented with increased miR-92a-3p expression as well as decreased KLF2 expression in PACs. The downregulation of miR-92a-3p and overexpression of KLF2 led to decline in expression of nuclear factor-κB (NF-κB), survivin, tumor necrosis factor-α, and Bax as well as extent of NF-κB phosphorylation, contents of inflammatory factors, and apoptosis rate of PACs, but to increased KLF2 and B-cell lymphoma-2 levels and proliferation rate of PACs. Collectively, the data obtained from the present study demonstrated that reduced miR-92a-3p expression may relieve AP through its suppressive effects on cell apoptosis,

Abbreviations: ANOVA, one-way analysis of variance; AP, acute pancreatitis; BCA, bicinchoninic acid; CRC, colorectal cancer; DAB, diaminobenzidine; DMEM, Dulbecco's modified Eagle's medium; ECL, chemiluminescence; EDTA, ethylenediaminetetraacetic acid; EdU, 5-ethynyl-2′-deoxyuridine; ELISA, enzyme-linked immunosorbent assay; FBS, fetal bovine serum; FITC, fluorescein isothiocyanate; GAPDH, glyceraldehyde-3-phosphate dehydrogenase; HE, hematoxylin-eosin; HEK, human embryo kidney; HRP, horseradish peroxidase; IgG, immunoglobulin G; KLF2, Kruppel-like factor 2; LPS, liposarcoma; miRNAs, microRNAs; mut, mutant type; NC, negative control; PACs, pancreatic acinar cells; PBS, phosphate buffered saline; PF, pulmonary fibrosis; PI, propidium iodide; RT-qPCR, reverse transcription quantitative polymerase chain reaction; SD, Sprague-Dawley; SDS-PAGE, sodium dodecyl sulfate-polyacrylamide gel electrophoresis; SP, streptavidin-peroxidase; TLRs, toll-like receptors; UTR, untranslated region; wt, wild type.

Lan Ling and Hai-Feng Wang contributed equally to this study.

inflammatory factors, and facilitatory effects on cell proliferation by enhancing KLF2 expression.

KEYWORDS

acute pancreatitis, apoptosis, Kruppel-like factor 2, microRNA-92a-3p, pancreatic acinar cells, proliferation

1 | INTRODUCTION

Acute pancreatitis (AP) is recognized as a common gastrointestinal emergency with an annual incidence of 0.005% to 0.08% as well as an overall mortality rate of 10% to 15%.[1] A majority of AP patients recover uneventfully within a few days, but still 20% of AP patients suffer from complications resulting from major infection, leading to 15% mortality.[2] Multiple risk factors have been reported to contribute to the occurrence and development of AP, including smoking, aging, gallstone, metabolic factors, alcoholism, and anatomic abnormalities.[3] Currently, organ supportive measures are the conventional treatment methods for organ failure, while debridement or drainage as well as antibodies are commonly used for the infected pancreatic necrosis; however, there is still no pharmacologic therapy effectively proven to mitigate AP.[4] With the technological advancement in genetic studies, an increasing number of microRNAs (miRNAs) have been reported to be associated with AP in rat and human,[5] yet the specific mechanism remains unknown.

miRNAs are a group of endogenous small noncoding RNAs that regulate translation of various target mRNAs, involving in most cellular and developmental processes as a novel and potent gene expression regulator.[6] It has been reported that some miRNAs, such as miR-24, miR-127 and miR-141, are involved in the regulation of AP.[7-9] Specifically, miR-92a-3p is a member of the miR-17 to 92 family, which is implicated in regulating cell metastasis, apoptosis, and viability.[10] A recent study has revealed that miR-92a-3p plays a crucial role in tumor growth and metastasis in gastric cancer by modulating cell apoptosis, migration, and proliferation.[11] In addition, the suppression of miR-92a-3p has been demonstrated to have an inhibitory effect on colorectal cancer (CRC) due to the suppression of cell proliferation as well as the enhancement of cell apoptosis and necrosis.[12] Kruppel-like factor 2 (KLF2), a member of the KLF family, has been recently identified as a tumor suppressor.[13] In addition, the regulatory role of KLF2 in the pathogenesis of certain inflammatory diseases has been elucidated by previous research.[14] Based on the aforementioned information, we hypothesized that miR-92a-3p and KLF2 may be involved in AP progression. Therefore, we performed this study to explore the molecular mechanism involved in miR-92a-3p affecting the onset and development of AP through regulating the KLF2 level.

2 | MATERIALS AND METHODS

2.1 | Ethics statement

This study was carried out in strict accordance with the recommendations provided by the Guide for the Care and Use of Laboratory Animals of the National Institutes of Health. The protocol was approved by the Institutional Animal Care and Use Committee of the China-Japan Friendship Hospital.

2.2 | Model establishment and grouping

A total of 40 male Sprague-Dawley rats of cleaning grade (weighing 225 ± 25 g) were purchased from the Shanghai Experimental Animal Center of Chinese Academy of Sciences (Shanghai, China). Twenty rats were subjected to the sham operation (sham-operated rats) with the remaining 20 rats injected using sodium taurocholate in a retrograde manner to establish the rat model for AP.[15] AP rats were fasted, and provided with free access to water 12 hours before the model establishment. The rats were injected using 40 mg/kg pentobarbital sodium (Beijing Biolab Science and Technology Co, Ltd, Beijing, China), set on the table, conventionally shaved, disinfected, and draped. Laparotomy was then conducted on the midline incision. The dodecadactylon and caput pancreatic were dually exposed, with a No. 5 needle inserted to drill a hole in the mesenteric blood vessel. A catheter was subsequently inserted into the dodecadactylon through a freshly constructed hole located toward the direction of the caput pancreatic in a retrograde way. The duct end was temporarily nipped by a micro-vessel clamp and the tube end was connected with the transfusion converter. Then, approximately 3% sodium taurocholate (0.1 mL/100 g, 115903, Shanghai JK Chemical Co, Ltd, Shanghai, China) was retrogradely injected into rats at a speed of 0.2 ml/min via the microinjection pump (Angel Electronic Equipment Co, Ltd, Shanghai, China). The micro-vessel clamp and catheter were subsequently

removed 4 to 5 minutes following the injection, while the hole in the lateral wall of the duodenum was sutured. In the sham-operated rats, only an exploratory laparotomy was conducted, void of the retrograde injection of sodium taurocholate. Twelve hours following the model establishment, 0.5–1.0 mL of blood was extracted using a 1 mL injector from the inferior vena cava of rats. The blood was centrifuged at the speed of 3000*g* for 10 minutes to isolate the serum. The isolated serum amylase activity was further evaluated with a kit (Nanjing Jiancheng Bioengineering Institute, Nanjing, Jiangsu, China) to verify whether the rat model of AP was established successfully.

2.3 | Hematoxylin-eosin (HE) staining

The pancreas tissues of the sham-operated rats and AP rats were soaked in 10% neutral buffered formalin, and then prepared into paraffin sections. The samples were subsequently dehydrated with alcohol, cleared twice with xylene, embedded in paraffin, and sliced into 4-μm sections. Next, the sections were dehydrated by using a gradient alcohol followed by clearance by xylene. Then, the sections were stained using hematoxylin (H8070-5g; Beijing Solarbio Science & Technology Co, Ltd, Beijing, China) for a total of 3 minutes, differentiated by hydrochloric acid-ethanol for 10 seconds, treated by ammonia water for 10 minutes, and stained with eosin solution (PT001; Shanghai Bogoo Biological Technology Co, Ltd, Shanghai, China) for a few seconds. Subsequently, the sections were then dehydrated, cleared, mounted, and observed under an optical microscope (DMM-300D; Shanghai Caikon Optical Instrument Co, Ltd, Shanghai, China).

2.4 | Masson trichrome staining

The sections were conventionally deparaffinized, stained with Ponceau S (RTD6301; Real-Times Beijing Biotechnology Co, Ltd, Beijing, China) for 2 minutes, 5% phosphomolybdic acid (P1910-100G; Shanghai Ruji Biotechnology Co, Ltd, Shanghai, China) solution for 2 minutes, and methyl green (BI005; Shanghai Ruji Biotechnology Co, Ltd) for 3 minutes. Then, the sections were treated using 95% alcohol for color separation, dehydrated by 100% alcohol, cleared by xylene, and sealed using neutral balsam. The collagen fiber was subsequently stained blue green, while the muscle fiber was stained pink.

2.5 | Immunohistochemistry

The tissue sections were deparaffinized and incubated with 3% H_2O_2 at room temperature for 15 minutes to eliminate the endogenous peroxidase. The sections were then treated using 0.01 mol/L citrate buffer solution (pH 6.0) in a microwave oven for a total of 10 minutes to repair the antigen, blocked using a 5% normal goat serum at room temperature for 15 minutes following the cool down, and finally cultured at 4°C overnight with the primary rabbit polyclonal antibody to KLF2 (1:100, ab203591; Abcam Inc, Cambridge, UK). Then, the previous sections were added the biotinylated goat anti-rabbit immunoglobulin G (IgG, 1:1000, ab6721; Abcam Inc), and cultured using horseradish peroxidase (HRP)-conjugated streptavidin for 15 minutes. Afterwards, the sections were treated with diaminobenzidine (DAB) solution for 3 to 5 minutes, counterstained using hematoxylin for 1 to 3 minutes, conventionally dehydrated, cleared, and sealed with neutral balsam. The steps mentioned above were repeated with 0.1 mol/L phosphate buffered saline (PBS) (pH 7.4) serving as a negative control (NC). Finally, the sections were grouped randomly, observed and photographed under a Primo Star digital microscope (Motic China Group Co, Ltd, Guangzhou, Guangdong, China). The yellow nucleus was regarded as a positive result. Five high-powered fields were observed continuously in each section, while the amounts of positive cells and negative cells in each high-power field were evaluated separately. The streptavidin-peroxidase (SP) staining kit was subsequently purchased from Shanghai Bluegene Biotech Co, Ltd (Shanghai, China), while the DAB kit was purchased from Beijing Zhongshan Goldenbridge Biotechnology Co, Ltd (Beijing, China).

2.6 | Dual-luciferase reporter gene assay

The human embryo kidney (HEK) 293T cells (China Center for Type Culture Collection, Wuhan, Hubei, China) were cultured in Dulbecco's modified Eagle's medium (DMEM) containing 10% fetal bovine serum (FBS) with 5% CO_2 at 37°C. The KLF2 3′-untranslated region (3′-UTR) fragment with the miR-92a-3p binding site was inserted into pmirGLO vector. The KLF2 3′-UTR fragment with the mutated binding site was constructed by the site-specific mutagenesis method and inserted into pmirGLO vector. The validity of the insertion sequence was verified by sequencing. The pmirGLO-wild type (wt) KLF2/pmirGLO-mutant type (mut)KLF2 recombinant vectors and miR-92a-3p mimic/mimic-NC were cotransfected into HEK-293T cells via the liposome transfection method. Next, 100 μL supernatant of lysate was mixed with 100 μL of renilla luciferase or firefly luciferase working solution to determine the activity of renilla luciferase or firefly luciferase. The multifunctional microplate reader SpectraMaxM5 (Molecular Devices Inc, Shanghai, China) was subsequently used to

determine the activities of renilla luciferase and firefly luciferase.

2.7 | Cellular model of AP establishment in vitro

The AR42J cell line, providing the same functions as pancreatic acinar cells (PACs) in normal rats, was used as study subjects. The cerulein was used to stimulate the AR42J cell lines for the AP cell model establishment in vitro.[16] The AR42J PACs of rats were purchased from the China Center for Type Culture Collection (Wuhan, Hubei, China). The AR42J cells were later preserved in Ham's F-12 medium (Invitrogen, Thermo Fisher Scientific Inc, Waltham, MA) containing 10% FBS (Sijiqing Bioengineering Materials Co, Ltd, Hangzhou, Zhejiang, China), 100 U/mL penicillin, and 100 μ/mL streptomycin. The cells were later seeded into a six-well plate at a rate of 1×10^5 cells/mL and incubated in a 37°C with 95% air and 5% CO_2. A total of 100 nM cerulein (Sigma-Aldrich Chemical Company, St Louis, MO) was dissolved in PBS to undergo AR42J cell treatment, and AR42J cells for control were treated solely with PBS. The cells were further incubated in an incubator for 24 hours, followed by collection of the cells and supernatant, and finally, three replicated wells were set in each group.

2.8 | Cell grouping and transfection

The AR42J cells were then stimulated by cerulein, followed by transfection with mimic-NC plasmids, miR-92a-3p mimic plasmids, inhibitor-NC plasmids, miR-92a-3p inhibitor plasmids, sh-NC plasmids, sh-KLF2 plasmids, oe-NC plasmids, oe-KLF2 plasmids, andcotransfected with inhibitor-NC and sh-KLF2 plasmids, miR-92a-3p inhibitor and sh-KLF2 plasmids, miR-92a-3p mimic and oe-NC plasmids, and miR-92a-3p mimic and oe-KLF2 plasmids, respectively, and AR42J cells with no treatment and no transfection were selected as controls. All the target plasmids mentioned above were purchased from Dharmacon Company (Lafayette, CO). The PACs were seeded in a 12-well plate at a density of 3×10^5 cells in each well. When the cell confluence finally reached 80%, transfection was conducted using the Lipofectamine 2000 kit (11668019; Invitrogen, Thermo Fisher Scientific Inc).

2.9 | Reverse transcription quantitative polymerase chain reaction

The total RNAs of pancreas tissues and PACs in each group were extracted using TRIzol reagent (Invitrogen, Carlsbad, CA). The Primescript RT reagent Kit (RRO37A; Takara, Tokyo, Japan) was used for reverse transcription. After successful reverse transcription, a fluorescence quantitative PCR instrument (ABI7500; Applied Biosystems Inc, Carlsbad, CA) was employed to amplify the target gene and internal control gene. The U6 served as an internal control of miR-92a-3p, while the glyceraldehyde-3-phosphate dehydrogenase (GAPDH) served as an internal control of other factors. The miR-92a-3p expression and mRNA levels of KLF2, survivin, tumor necrosis factor-α (TNF-α), Bcl-2-associated X protein (Bax), and B-cell CLL/Lymphoma 2 (Bcl-2) were calculated using the $2^{-\Delta\Delta C_t}$ method.[17] The primer sequences are shown in Table 1.

2.10 | Western blot analysis

The total proteins of PACs were extracted using a protein lysis buffer (C0481; Sigma-Aldrich Chemical Company, St Louis, MO), while the bicinchoninic acid assay was conducted for protein quantification. After 10% sodium dodecyl sulfate-polyacrylamide gel electrophoresis, proteins were transferred onto a nitrocellulose membrane, and incubated at 4°C overnight with the following rabbit polyclonal antibodies to KLF2 (1:100, ab203591), NF-κB (1:500, ab16502), NF-κB phosphorylation (1:500, ab28856), survivin (1:1000, ab469), TNF-α (1:500, ab6671), Bax (1:500, ab53154), and Bcl-2 (1:500, ab196495). On the following day, the membrane was washed three times using tris-buffered saline Tween (TBST) (5 minutes each time), incubated for 1.5 hours using goat anti-rabbit HRP-labeled IgG (1:2000, ab205718) (all antibodies were purchased from Abcam Inc), and washed with TBST. The enhanced chemiluminescence reagent (NCI4106; Pierce, Rockford, IL) was used for the observation of protein levels. The steps mentioned above were repeated with GAPDH serving as the internal control. Image J (Bio-Rad, Inc, Hercules, CA) software was used for gray value analysis.

2.11 | 5-Ethynyl-2′-deoxyuridine staining

PACs in the logarithmic growth phase were seeded in a 96-well plate at 4×10^3 to 1×10^5 cells/well and cultured to normal growth phase. The proliferation of PACs was detected by the 5-ethynyl-2′-deoxyuridine (EdU) cell proliferation detection kit (C10310-1/-2/-3).

2.12 | Flow cytometry

The cells were treated with an ethylenediaminetetraacetic acid-free trypsin at the 48th h following cell transfection, and centrifuged. The apoptosis of the cells was detected

TABLE 1 Primer sequences for RT-qPCR

Gene	Primer sequence
miR-92a-3p	F: 5′-GGGGCAGTTATTGCACTTGTC-3′ R: 5′-CCAGTGCAGGGTCCGAGGTA-3′
KLF2	F: 5′-ACTTGCAGCTACACCAACTG-3′ R: 5′-CTGTGACCCGTGTGCTTG-3′
survivin	F: 5′-CAACCTGGACCTGAGTGACAT-3′ R: 5′-CCACCCATAGATCCTGTCAGA-3′
TNF-α	F: 5′-GAACAACCCTACGAGCACCT-3′ R: 5′-GGGTAGTTTGGCTGGGATAA-3′
Bax	F: 5′-AACAACATGGAGCTGCAGAGG-3′ R: 5′-GAAGTTGCCGTCTGCAAACAT-3′
Bcl-2	F: 5′-GGGATGACTTCTCTCGTCGCTAC-3′ R: 5′-GTTGTCCACCAGGGGTGACAT-3′
GAPDH	F: 5′-TGGTATCGTGGAAGGACTCAT--3′ R: 5′-GTGGGTGTCGCTGTTGAAGTC-3′
U6	F: 5′-GACACGCAAATTCGTGAAGCG-3′ R: 5′-TCCAGTGCAGGGTCCGAG-3′

Abbreviations: Bax, Bcl2-associated X protein; Bcl-2, B-cell lymphoma-2; F, forward; GAPDH, glyceraldehyde-3-phosphate dehydrogenase; KLF2, Kruppel-like factor 2; miR-92a-3p, microRNA-92a-3p; NC, negative control; R, reverse; RT-qPCR, reverse transcription quantitative polymerase chain reaction; TNF-α, tumor necrosis factor-α.

using the annexin-V-fluorescein isothiocyanate (FITC)/propidium iodide (PI) apoptosis detection kit (CA1020; Beijing Solarbio Science & Technology Co, Ltd, Beijing, China), The cells were subsequently washed with binding buffer, re-suspended by Annexin-V-FITC and binding buffer mixed at 1:40, and incubated for 30 minutes. Then, the PI and binding buffer were mixed at 1:40, and incubated with cells for 15 minutes. The flow cytometer was employed to detect the apoptosis of cells.

2.13 | Enzyme-linked immunosorbent assay

Cells from each group were subsequently seeded in a 12-well plate and cultured for 48 hours, with the supernatant being collected to determine the contents of TNF-α (69-99985), interleukin-6 (IL-6) (69-99854), IL-2 (69-99852), and IL-1β (69-59812) in the supernatant. The specific steps were taken in accordance with the instructions provided by the kits. The kits were purchased from MSK Biotech Corp (Wuhan, Hubei, China).

2.14 | Statistical analysis

Statistical analysis was conducted by using SPSS 21.0 (IBM Corp, Armonk, NY). Measurement data were expressed as mean ± standard deviation. Initially, the normality and homogeneity of variance test was carried out, with the data in normal distribution and the homogeneity of variance analyzed as follows: data differences between two groups were analyzed by unpaired *t* test, while the data among multiple groups were analyzed by one-way analysis of variance. The rank sum test was performed if data did not conform to normal distribution or homogeneity of variance. A $P < .05$ was considered statistically significant.

3 | RESULTS

3.1 | Rat model of AP is successfully established and miR-92a-3p is highly expressed while KLF2 is poorly expressed in the pancreas tissues of AP rats

The amylase activity in the serum of sham-operated rats AP rats were determined to identify whether the rat model of AP had been established successfully. The results showed that 12 hours following model establishment, 15 AP rats had presented with higher activity of amylase in serum than the sham-operated rats (Figure 1A), with the success rate of model establishment being 75%. Subsequently, 12 rats were randomly selected from the 20 sham-operated rats and the 15 AP rats, respectively, for the subsequent experiments.

Hematoxylin-eosin (HE) staining and Masson trichrome staining were performed to observe the detailed differences in pancreas tissues of sham-operated rats and AP rats. The results of the HE staining shown in Figure 1B suggested that edema, infiltration of inflammatory cells, and necrosis of PACs were not observed in pancreas tissues of sham-operated rats; while the pancreas tissues of the AP rats displayed edematous PACs, necrosis of varying degrees in multiple places, and a great quantity of infiltration and bleeding of inflammatory cells. The results of Masson trichrome staining (Figure 1C) revealed that the pancreas tissues of the sham-operated rats looked normal, while the pancreas tissues of the AP rats appeared dark in color, which were also accompanied by a large number of blue-green collagenous fiber and collagen deposition.

Reverse transcription quantitative polymerase chain reaction (RT-qPCR) and immunohistochemistry were performed together to determine the expression of miR-92a-3p and KLF2 in the pancreas tissues of sham-operated rats and AP rats. The results of the RT-qPCR (Figure 1D) showed that when compared with the sham-operated rats, the miR-92a-3p expression became elevated in AP rats ($P < .05$), suggesting that miR-92a-3p is highly expressed in the pancreas tissues of AP rats. The results of immunohistochemistry (Figures 1E and 1F) indicated that the positive rate of KLF2 protein in the pancreas tissues of

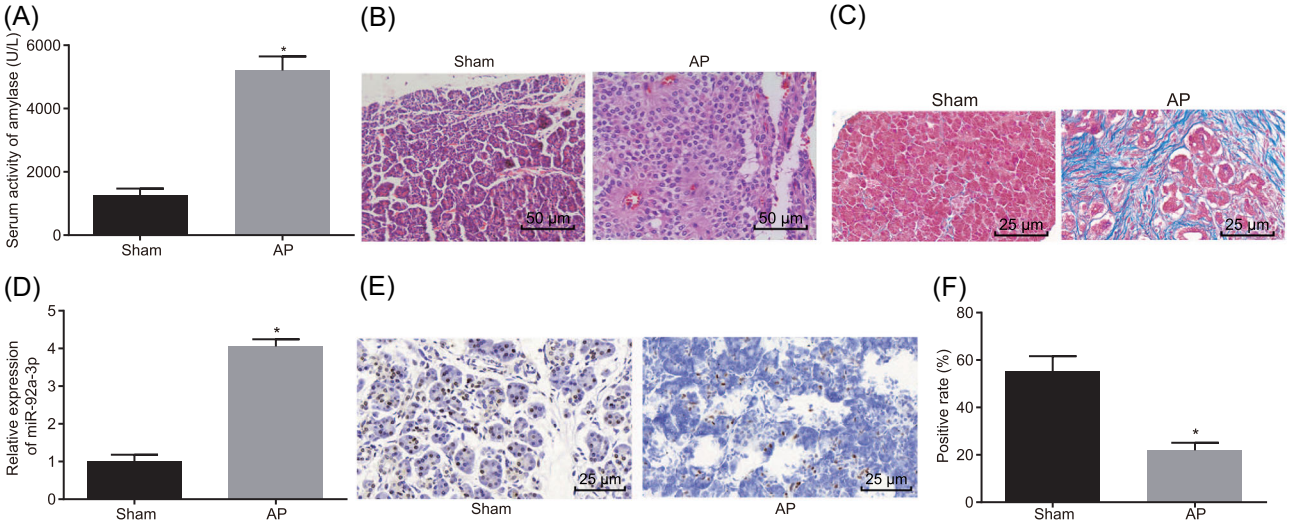

FIGURE 1 Rat model of AP is successfully developed and pancreatic tissues of AP rats exhibit upregulated miR-92a-3p and downregulated KLF2. A, amylase activity in serum of sham-operated rats and the AP rats. *$P < .05$ vs the sham-operated rats; n = 20. B, Pathological changes of pancreas tissues of sham-operated rats and AP rats detected by HE staining (×200). C, Pathological changes of pancreas tissues of sham-operated rats and AP rats detected by Masson trichrome staining (×400). D, miR-92a-3p expression in pancreas tissues of sham-operated rats and AP rats determined by RT-qPCR. E, Positive expression of KLF2 in pancreas tissues of sham-operated rats and AP rats detected by immunohistochemistry (×400). F, Positive rates of KLF2 in pancreas tissues of sham-operated rats and AP rats; n = 12. The measurement data were expressed as mean ± standard deviation; the data of each group were analyzed by unpaired *t* test. AP, acute pancreatitis; HE, hematoxylin-eosin; KLF2, Kruppel-like factor 2; miR-92a-3p, microRNA-92-3p; RT-qPCR, reverse transcription quantitative polymerase chain reaction. *$P < .05$ vs the sham-operated rats

AP rats was 21.91%, which was lower than the 55.11% in the sham-operated rats ($P < .05$). These results demonstrated that AP rats had high miR-92a-3p level and low KLF2 level in the pancreas tissues.

3.2 | KLF2 is a target gene of miR-92a-3p

According to the biological prediction website microRNA.org, there was a specific binding region between KLF2 3′UTR and the miR-92a-3p sequence, as shown in Figure 2A. To further prove that miR-92a-3p targeted KLF2, the dual-luciferase reporter assay was conducted, with the results shown in Figure 2B. The luciferase activity of the cells cotransfected with miR-92a-3p mimic and KLF2-wt was lower than the activity observed in the mimic-NC group ($P < .05$), with no significant change determined in the luciferase activity of cells transfected with miR-92a-3p mimic and KLF2-mut plasmids ($P > .05$). These results demonstrated that KLF2 is a target gene of miR-92a-3p.

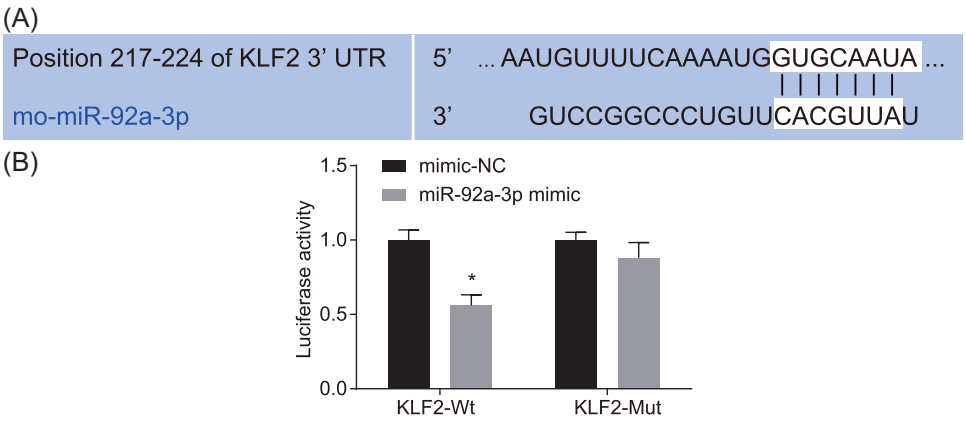

FIGURE 2 miR-92a-3p targets at 3′-UTR of KLF2. A, sequences of 3′-UTR of KLF2; B, luciferase activities of cells transfected with different plasmids determined by dual-luciferase reporter gene assay; the statistical data were expressed as mean value of standard error; the data of each group were analyzed by unpaired *t* test; the experiments were conducted three times. KLF2, Kruppel-like factor 2; miR-92a-3p, microRNA-92a-3p; NC, negative control; 3′-UTR, 3′-untranslated region. *$P < .05$ vs the mimic-NC group

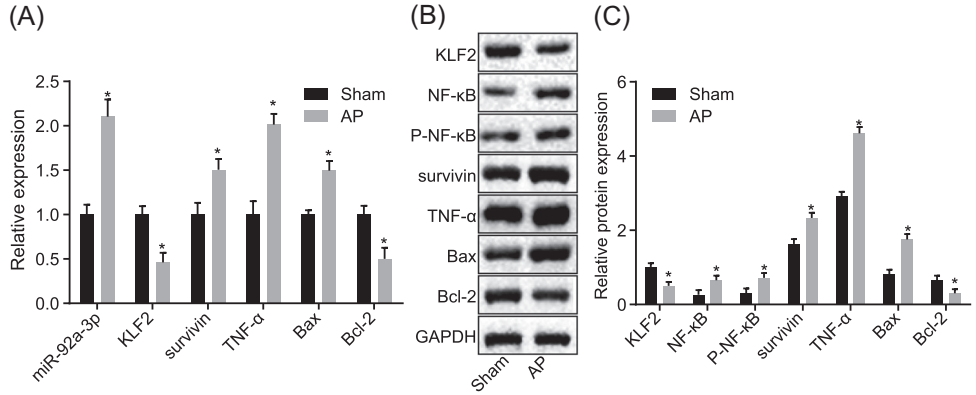

FIGURE 3 miR-92a-3p reduces KLF2 expression in PACs of AP. A, miR-92a-3p expression and the mRNA levels of KLF2, survivin, TNF-α, Bax, and Bcl-2 in AR42J cells without treatment and cerulein-treated AR42J cells determined by RT-q-PCR; B, the gray value of KLF2, NF-κB, survivin, TNF-α, Bax, and Bcl-2 as well as the extent of NF-κB phosphorylation protein bands in AR42J cells without treatment and cerulein-treated AR42J cells detected by Western blot analysis; C, protein levels of KLF2, NF-κB, survivin, TNF-α, Bax, and Bcl-2 as well as the extent of NF-κB phosphorylation in AR42J cells without treatment and cerulein-treated AR42J cells; the statistical data were expressed as mean value standard error; the data of each group were analyzed by unpaired *t* test; the experiments were conducted three times. AP, acute pancreatitis; Bax, Bcl2-associated X protein; Bcl-2, B-cell lymphoma-2; KLF2, Kruppel-like factor 2; miR-92a-3p, microRNA-92a-3p; NF-κB, nuclear factor-κB; PAC, pancreatic acinar cell; TNF-α, tumor necrosis factor-α. *$P < .05$, vs the AR42J cells without treatment

3.3 | miR-92a-3p is highly expressed and KLF2 is poorly expressed in PACs

The AR42J cells were stimulated by cerulein to induce the cellular model of AP in vitro, after which RT-qPCR (Figure 3A) and Western blot analysis (Figures 3B and 3C) were performed to evaluate the expression of miR-92a-3p, NF-κB, survivin, TNF-α, Bax, Bcl-2, and KLF2 as well as the extent of NF-κB phosphorylation in AR42J cells without transfection and cerulein-treated AR42J cells. The expression of miR-92a-3p, NF-κB, survivin, TNF-α, and Bax as well as the extent of NF-κB phosphorylation increased, while the KLF2 and Bcl-2 decreased in cerulein-treated AR42J cells versus the AR42J cells without transfection.

3.4 | Downregulation of miR-92a-3p suppresses AP progression by increasing KLF2 levels

RT-qPCR (Figure 4A) and Western blot analysis (Figures 4B and 4C) indicated that the cerulein-treated AR42J cells transfected with miR-92a-3p mimic had higher NF-κB, survivin, TNF-α, and Bax expression as well as the extent of NF-κB phosphorylation and lower KLF2 and Bcl-2 expression, while cells transfected with miR-92a-3p inhibitor had the opposite trends.

3.5 | Increased KLF2 suppresses related gene expression

RT-qPCR (Figure 5A) and Western blot analysis (Figures 5B and 5C) revealed that the expression of NF-κB, survivin, TNF-α, and Bax as well as the extent of NF-κB phosphorylation was elevated in cerulein-treated AR42J cells transfected with sh-KLF2, yet the expression of KLF2 and Bcl-2 descreased. Contrarily, the cerulein-treated AR42J cells transfected with oe-KLF2 showed the opposite results.

3.6 | Downregulated miR-92a-3p elevates KLF2 to suppress AP progression

RT-qPCR (Figure 6A) and Western blot analysis (Figures 6B and 6C) suggested that the expression of NF-κB, survivin, TNF-α, and Bax as well as the extent of NF-κB phosphorylation in cerulein-treated AR42J cells cotransfected with miR-92a-3p inhibitor and sh-KLF2 were decreased, while the KLF2 and Bcl-2 expression showed an increasing trend ($P < .05$) in comparison with the cerulein-treated AR42J cells cotransfected with inhibitor-NC and sh-KLF2. Similarly, cerulein-treated AR42J cells cotransfected with miR-92a-3p mimic and oe-KLF2 had higher Bcl-2 and KLF2 expression, along with reduced NF-κB, survivin, TNF-α, and Bax expression as well as extent of NF-κB phosphorylation. These results further demonstrate that inhibition of miR-92a-3p has the potential to suppress AP progression by promoting KLF2 expression.

3.7 | Downregulated miR-92a-3p suppresses apoptosis but improves proliferation of PACs by promoting KLF2 expression

EdU staining and flow cytometry were performed to detect the proliferation and apoptosis of PACs in AP rats. The proliferation rate of cerulein-treated AR42J cells

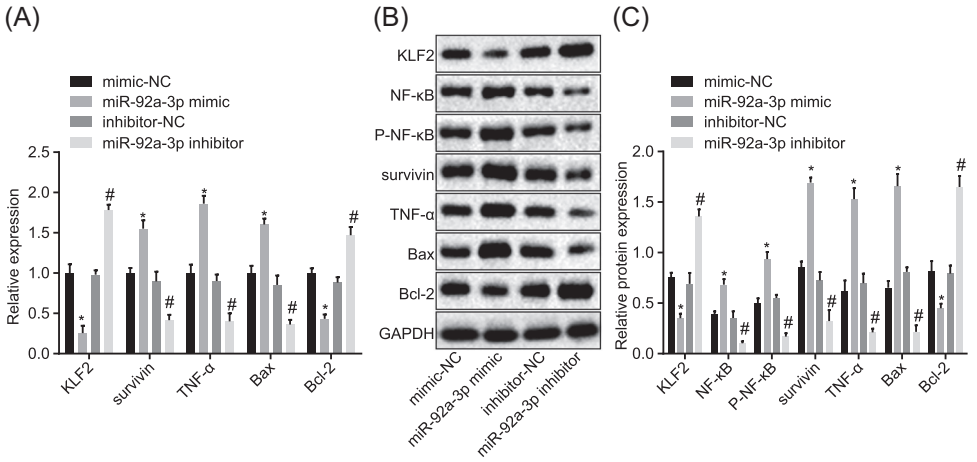

FIGURE 4 Reduced miR-92a-3p promotes related gene expression in PACs. A, mRNA levels of KLF2, survivin, TNF-α, Bax, and Bcl-2 in cerulein-treated AR42J cells treated with mimic-NC, miR-92a-3p mimic, inhibitor-NC, or miR-92a-3p inhibitor, as determined by RT-qPCR; B, the gray value KLF2, NF-κB, survivin, TNF-α, Bax, and Bcl-2 as well as the extent of NF-κB phosphorylation protein band in cerulein-treated AR42J cells treated with mimic-NC, miR-92a-3p mimic, inhibitor-NC, or miR-92a-3p inhibitor, as assessed by Western blot analysis; C, protein levels of KLF2, NF-κB, survivin, TNF-α, Bax, and Bcl-2 as well as the extent of NF-κB phosphorylation in cerulein-treated AR42J cells treated with mimic-NC, miR-92a-3p mimic, inhibitor-NC, or miR-92a-3p, as evaluated by Western blot analysis; the statistical data were expressed as mean value of standard error and analyzed by one-way ANOVA; the experiments were conducted three times. ANOVA, analysis of variance; Bax, Bcl2-associated X protein; Bcl-2, B-cell lymphoma-2; KLF2, Kruppel-like factor 2; miR-92a-3p, microRNA-92a-3p; NC, negative control; NF-κB, nuclear factor-κB; PAC, pancreatic acinar cell; TNF-α, tumor necrosis factor-α. $^{*}P < .05$ vs the cerulein-treated AR42J cells treated with mimic-NC; $^{\#}P < .05$ vs the cerulein-treated AR42J cells treated with inhibitor-NC

transfected with miR-92a-3p mimic dropped, while the apoptosis rate increased, which could be reversed by miR-92a-3p inhibitor transfection (Figure 7A). In addition, the proliferation rate of cerulein-treated AR42J cells transfected with sh-KLF2 dropped, while the apoptosis rate was elevated. However, cerulein-treated AR42J cells transfected with oe-KLF2 presented the opposite trend (Figure 7B). Furthermore, the proliferation rate of cerulein-treated AR42J cells cotransfected with miR-92a-3p inhibitor and sh-KLF2 was elevated, while the apoptosis rate dropped, however, this can be blocked in cerulein-treated AR42J cells cotransfected with

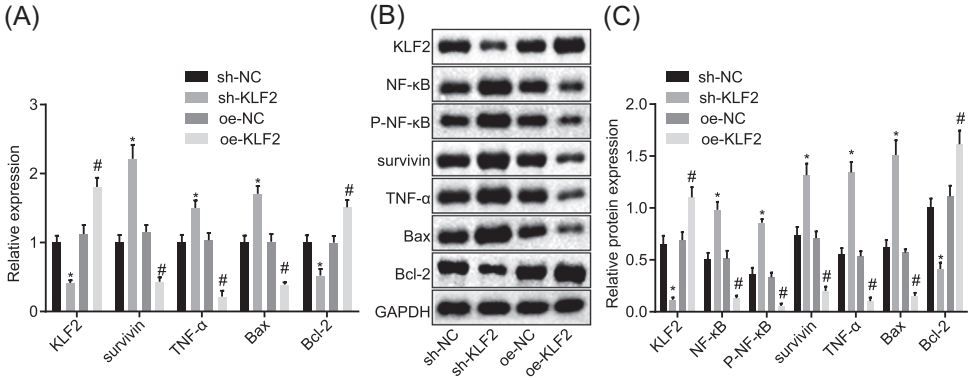

FIGURE 5 KLF2 inhibits NF-κB, survivin, TNF-α, and Bax expression as well as the extent of NF-κB phosphorylation but increases Bcl-2 expression in PACs of rats. A, mRNA levels of KLF2, survivin, TNF-α, Bax, and Bcl-2 in cerulein-treated AR42J cells treated with sh-NC, sh-KLF2, oe-NC, or oe-KLF2 determined by RT-qPCR. B, The gray value of KLF2, NF-κB, survivin, TNF-α, Bax, and Bcl-2 as well as the extent of NF-κB phosphorylation protein bands in cerulein-treated AR42J cells treated with sh-NC, sh-KLF2, oe-NC, or oe-KLF2, as tested by Western blot analysis. C, Protein levels of KLF2, NF-κB, survivin, TNF-α, Bax, and Bcl-2 as well as the extent of NF-κB phosphorylation in cerulein-treated AR42J cells treated with sh-NC, sh-KLF2, oe-NC, or oe-KLF2; the statistical data were expressed as mean value of standard error and analyzed by one-way ANOVA; the experiments were conducted three times. ANOVA, analysis of variance; Bax, Bcl2-associated X protein; Bcl-2, B-cell lymphoma-2; KLF2, Kruppel-like factor 2; miR-92a-3p, microRNA-92a-3p; NC, negative control; NF-κB, nuclear factor-κB; PAC, pancreatic acinar cell; TNF-α, tumor necrosis factor-α. $^{*}P < .05$ vs the cerulein-treated AR42J cells treated with sh-NC; $^{\#}P < .05$ vs the cerulein-treated AR42J cells treated with oe-NC

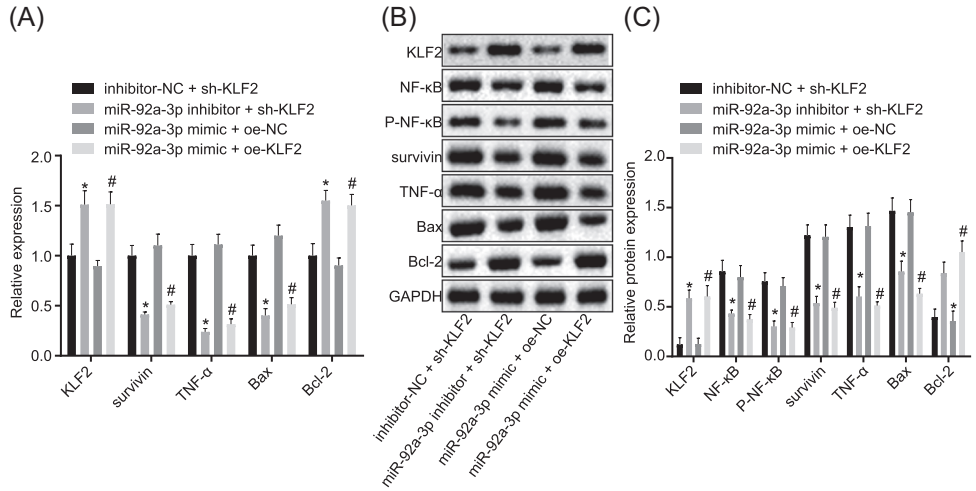

FIGURE 6 Depletion of miR-92a-3p suppress AP development by increasing the expression of KLF2. A, mRNA levels of KLF2, survivin, TNF-α, Bax, and Bcl-2 in cerulein-treated AR42J cells co-treated with inhibitor-NC and sh-KLF2, miR-92a-3p inhibitor and sh-KLF2, miR-92a-3p mimic and oe-NC, or miR-92a-3p mimic and oe-KLF2 determined by RT-qPCR. B, Gray value of KLF2, NF-κB, survivin, TNF-α, Bax, and Bcl-2 as well as the extent of NF-κB phosphorylation protein bands in cerulein-treated AR42J cells co-treated with inhibitor-NC and sh-KLF2, miR-92a-3p inhibitor and sh-KLF2, miR-92a-3p mimic and oe-NC, or miR-92a-3p mimic and oe-KLF2 detected by Western blot analysis. C, Protein levels of KLF2, NF-κB, survivin, TNF-α, Bax, and Bcl-2 as well as the extent of NF-κB phosphorylation in cerulein-treated AR42J cells co-treated with the inhibitor-NC and sh-KLF2, miR-92a-3p inhibitor and sh-KLF2, miR-92a-3p mimic and oe-NC or miR-92a-3p mimic and oe-KLF2; the statistical data were expressed as mean value of standard error and analyzed by one-way ANOVA; the experiments were conducted three times. ANOVA, analysis of variance; Bax, Bcl2-associated X protein; Bcl-2, B-cell lymphoma-2; KLF2, Kruppel-like factor 2; miR-92a-3p, microRNA-92a-3p; mRNA, messenger RNA; NF-κB, nuclear factor-κB; RT-qPCR, reverse transcription quantitative polymerase chain reaction; TNF-α, tumor necrosis factor-α. $^{*}P < .05$ vs the cerulein-treated AR42J cells cotransfected with inhibitor-NC and sh-KLF2; $^{\#}P < .05$ vs the cerulein-treated AR42J cells cotransfected with miR-92a-3p mimic and oe-NC

miR-92a-3p mimic and oe-KLF2 (Figure 7C). Collectively, these findings suggested that the suppression of miR-92a-3p upregulates KLF2 expression, thus inhibiting apoptosis and promoting proliferation of PACs.

3.8 | Inhibited miR-92a-3p promotes KLF2 expression to suppresses expressions of inflammatory factors in PACs

Enzyme-linked immunosorbent assay (ELISA) was performed to evaluate the levels of inflammatory factors in PACs when miR-92a-3p and KLF2 were differentially modulated. Cerulein-treated AR42J cells transfected with miR-92a-3p mimic had higher TNF-α, IL-6, IL-2, and IL-1β levels. Contrarily, cerulein-treated AR42J cells transfected with the miR-92a-3p inhibitor had lower TNF-α, IL-6, IL-2, and IL-1β levels (Figure 8A). Similarly, the TNF-α, IL-6, IL-2, and IL-1β levels in cerulein-treated AR42J cells treated with sh-KLF2 increased obviously; however, the levels in cerulein-treated AR42J cells treated with oe-KLF2 showed significant reduction (Figure 8B). In addition, the aforementioned levels in cerulein-treated AR42J cells cotransfected with miR-92a-3p inhibitor and sh-KLF2 were decreased, and those with miR-92a-3p mimic and oe-KLF2 were also decreased (Figure 8C). These results revealed that the downregulated miR-92a-3p could reduce the expressions of inflammatory factors in PACs by elevating the expression of KLF2.

4 | DISCUSSION

AP, a severe inflammation of the pancreas, is recognized to originate from the injury of local acinar cells, and some other regional tissues as well as remote organ systems are involved in the process in different degrees.[18] The response of PACs to various risk factors including gallstones, hyperlipidemia, cigarette smoking, and alcohol abuse have also been recognized as the cause of pathologic events in AP.[19] Recently, some genes, including PRSS1, SPINK1, CFTR, chymotrypsin C, calcium-sensing receptor, and claudin-2, have been confirmed to be related with the progression of AP as its polymorphisms and mutations act as cofactors interacting with other causes.[20] In this study, we aimed to determine the mechanism by which miR-92a-3p affected the development of AP, and the results suggested that inhibition of miR-92a-3p can upregulate KLF2 expression to modulate inflammatory factors, and promote proliferation and suppress the apoptosis of PACs, thereby further inhibiting AP progression.

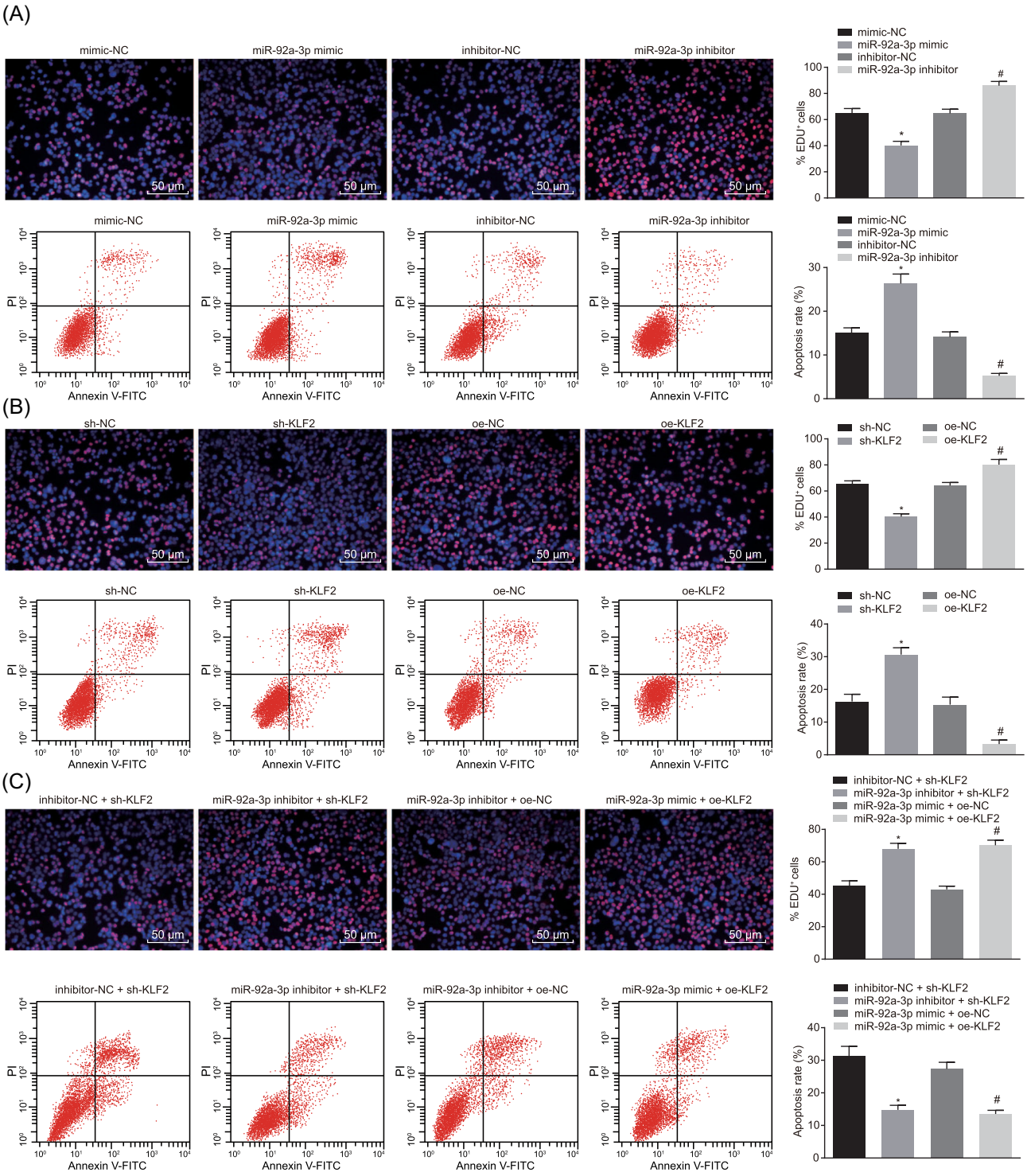

FIGURE 7 Reduced miR-92a-3p inhibits apoptosis but enhances proliferation of PACs by promoting KLF2 expression. A, apoptosis and proliferation of cerulein-treated AR42J cells treated with mimic-NC, miR-92a-3p mimic, inhibitor-NC, or miR-92a-3p inhibitor plasmids detected by EdU staining and flow cytometry. B, Apoptosis and proliferation of cerulein-treated AR42J cells treated with sh-NC, sh-KLF2, oe-NC, or oe-KLF2 plasmids detected by EdU staining and flow cytometry. C, Apoptosis and proliferation of cerulein-treated AR42J cells co-treated with inhibitor-NC and sh-KLF2, miR-92a-3p inhibitor and sh-KLF2, miR-92a-3p mimic and oe-NC, or miR-92a-3p mimic and oe-KLF2 plasmids detected by EdU staining and flow cytometry; the statistical data were expressed as mean value of standard error and analyzed by one-way ANOVA; the experiments were conducted three times. ANOVA, analysis of variance; EdU, 5-ethynyl-2′-deoxyuridine; KLF2, Kruppel-like factor 2; miR-92a-3p, microRNA-92a-3p; NC, negative control; PAC, pancreatic acinar cell. $^{*}P < .05$ vs the cerulein-treated AR42J cells transduced with mimic-NC or sh-NC or both inhibitor-NC and sh-KLF2; $^{\#}P < .05$ vs the cerulein-treated AR42J cells transduced with inhibitor-NC or oe-NC or both miR-92a-3p mimic and oe-NC

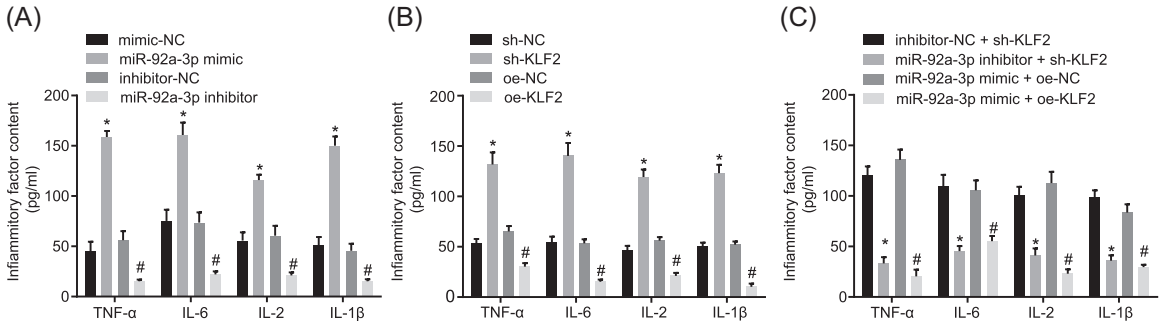

FIGURE 8 Decreased miR-92a-3p enhances KLF2 expression to inhibit expression of inflammatory factors in PACs. A, levels of inflammatory factors in the cerulein-treated AR42J cells treated with mimic-NC, miR-92a-3p mimic, inhibitor-NC, or miR-92a-3p inhibitor plasmids determined by ELISA. B, levels of inflammatory factors in the cerulein-treated AR42J cells treated with sh-NC, sh-KLF2, oe-NC, or oe-KLF2 plasmids determined by ELISA. C, Levels of inflammatory factors in the cerulein-treated AR42J cells co-treated with inhibitor-NC and sh-KLF2, miR-92a-3p inhibitor and sh-KLF2, miR-92a-3p mimic and oe-NC, or miR-92a-3p and oe-KLF2 plasmids determined by ELISA; the statistical data were expressed as mean value of standard error and analyzed by one-way ANOVA; the experiments were conducted three times. ELISA, enzyme-linked immunosorbent assay; KLF2, Kruppel-like factor 2; miR-92a-3p, microRNA-92a-3p; PAC, pancreatic acinar cell. $^{*}P < .05$ vs the cerulein-treated AR42J cells transfected with mimic-NC or sh-NC or both inhibitor-NC and sh-KLF2; $^{\#}P < .05$ vs the cerulein-treated AR42J cells transfected with inhibitor-NC or oe-NC or both miR-92a-3p mimic and oe-NC

Initially, we observed that the miR-92a-3p level was elevated in PACs. Moreover, when miR-92a-3p was downregulated, the apoptosis of PACs was inhibited; however, the proliferation was improved, suggesting that miR-92a-3p plays a key role in the genesis and development of AP. In addition to its role in AP, much literature has revealed the participation of miR-92a-3p in various diseases and even tumor progression. In specific terms, a previous report showed that miR-92a-3p is expressed at a high level in gastric cancer tissues, and is able to suppress cell apoptosis, and promote cell invasion, migration, and proliferation.[21] It has also been reported that the miR-92a-3p level is upregulated in the circulating exosomes of patients with CRC and participates in the tumorigenesis and metastasis of CRC.[22] Additionally, aberrant miR-92a-3p expression has been recognized as a booster of malignant glioma via promotion of cell invasion and proliferation, but attenuating cell apoptosis.[23] It was reported that treatment of miR-92a-3p inhibitor resulted in potentiated Wilms' tumor cell proliferation, migration, and invasion abilities.[24] Lucia Casadei et al[25] also reported that miR-92a-3p is implicated in the inflammatory process before tumorigenesis via triggering of the toll-like receptor response of the immune cells, thereby stimulating the development of liposarcoma in a paracrine manner. Altogether, significant evidence demonstrating that the decrease in miR-92a-3p is able to lessen the progression of AP by inhibiting apoptosis and promoting proliferation of PACs

The present study also demonstrated that PACs of AP rats exhibited lower KLF2 levels. In addition, based on the biological prediction website and luciferase activity determination, we found that KLF2 is a putative target gene of miR-92a-3p and is negatively regulated by it. KLF2, a member of the KLF family, has been demonstrated to play a crucial role in suppressing inflammation and pulmonary fibrosis by regulating AP-1.[26] According to a previous study, the KLF2 level decreased in pancreatic cancer, and the role of KLF2 in repressing carcinogenesis through the inhibition of metastasis, migration, and growth of cancer cells has been elucidated to provide a potential therapy strategy for the pancreatic cancer.[27] As detected by Zou et al,[28] overexpressed KLF2 promoted cell invasion and proliferation but attenuated cell apoptosis in hepatocellular carcinoma. Besides this, KLF2 is able to modulate the transcriptional activity of NF-κB, thus restraining the expression of some inflammatory genes.[14] In accordance with previous studies, our study demonstrated that the elevation of KLF2 level was associated with blocked inflammatory factors including NF-κB, survivin, TNF-α, and Bax. It has been well documented that high level of TNF-α, a pro-inflammatory mediator, can bring forth a feed-forward inflammatory response, resulting in the deterioration of AP, and its regulator, NF-κB, has also exacerbated AP when it is overexpressed.[29] The study conducted by Zhang et al[30] has revealed that survivin, which belongs to the inhibitor of apoptosis family, is upregulated in a number of cancers and plays a vital role in protecting cancer cells from apoptosis. The findings of this study suggested that decreased miR-92a-3p enhances KLF2 expression, and reduced the contents of inflammatory factors, leading to attenuated development of AP.

Based on these findings in the present study, we propose that downregulation of miR-92a-3p confers a remedial role by which miR-92a-3p downregulation improves the expression of KLF2, thus reducing the

contents of inflammatory factors, suppressing apoptosis and promoting proliferation of PACs. Therefore, miR-92a-3p may potentially serve as a therapeutic target for the AP treatment in the future. Further studies are required, however, to fully understand the specific mechanisms of miR-92a-3p combined with KLF2 and inflammatory factors on progression and development of AP. Moreover, it is expected to demonstrate the effects of miR-92a-3p and KLF2 on PACs based on different models of AP in future studies.

ACKNOWLEDGMENTS

The authors thank the reviewers for their helpful comments.

CONFLICT OF INTERESTS

The authors declare that there are no conflict of interests.

AUTHOR CONTRIBUTIONS

LL designed the study. JL and YL collated the data and carried out data analyses. H-FW and C-DG drafted the manuscript. LL, H-FW edited and revised manuscript. All authors have read and approved the final submitted manuscript.

DATA AVAILABILITY STATEMENT

The data that support the findings of this study are available from the corresponding author upon reasonable request.

ORCID

Cheng-Dong Gu http://orcid.org/0000-0002-9206-1040

REFERENCES

1. Mourad MM, Evans R, Kalidindi V, Navaratnam R, Dvorkin L, Bramhall SR. Prophylactic antibiotics in acute pancreatitis: endless debate. *Ann R Coll Surg Engl*. 2017;99:107-112. https://doi.org/10.1308/rcsann.2016.0355
2. Bakker OJ, van Brunschot S, van Santvoort HC, et al. Early versus on-demand nasoenteric tube feeding in acute pancreatitis. *N Engl J Med*. 2014;371:1983-1993. https://doi.org/10.1056/NEJMoa1404393
3. Chang CC, Chang YS, Wang SH, Lin SY, Chen YH, Chen JH. Primary Sjogren's syndrome and the risk of acute pancreatitis: a nationwide cohort study. *BMJ Open*. 2017;7):e014807. https://doi.org/10.1136/bmjopen-2016-014807
4. Kambhampati S, Park W, Habtezion A. Pharmacologic therapy for acute pancreatitis. *World J Gastroenterol*. 2014;20:16868-16880. https://doi.org/10.3748/wjg.v20.i45.16868
5. Blenkiron C, Askelund KJ, Shanbhag ST, et al. MicroRNAs in mesenteric lymph and plasma during acute pancreatitis. *Ann Surg*. 2014;260:341-347. https://doi.org/10.1097/SLA.0000000000000447
6. Sang HQ, Jiang ZM, Zhao QP, Xin F. MicroRNA-133a improves the cardiac function and fibrosis through inhibiting Akt in heart failure rats. *Biomed Pharmacother*. 2015;71:185-189. https://doi.org/10.1016/j.biopha.2015.02.030
7. Meng S, Wang H, Xue D, Zhang W. Screening and validation of differentially expressed extracellular miRNAs in acute pancreatitis. *Mol Med Rep*. 2017;16:6412-6418. https://doi.org/10.3892/mmr.2017.7374
8. Shi N, Deng L, Chen W, et al. Is MicroRNA-127 a Novel Biomarker for Acute Pancreatitis with Lung Injury? *Dis Markers*. 2017;2017:1204295. https://doi.org/10.1155/2017/1204295
9. Zhu H, Huang L, Zhu S, et al. Regulation of autophagy by systemic admission of microRNA-141 to target HMGB1 in l-arginine-induced acute pancreatitis in vivo. *Pancreatology*. 2016;16:337-346. https://doi.org/10.1016/j.pan.2016.03.004
10. Song H, Zhang Y, Liu N, Zhao S, Kong Y, Yuan L. miR-92a-3p exerts various effects in glioma and glioma stem-like cells specifically targeting CDH1/beta-catenin and notch-1/Akt signaling pathways. *Int J Mol Sci*. 2016;17:pii:E1799. https://doi.org/10.3390/ijms17111799
11. Zhang G, Li S, Lu J, et al. LncRNA MT1JP functions as a ceRNA in regulating FBXW7 through competitively binding to miR-92a-3p in gastric cancer. *Mol Cancer*. 2018;17:87. https://doi.org/10.1186/s12943-018-0829-6
12. Ahmadi S, Sharifi M, Salehi R. Locked nucleic acid inhibits miR-92a-3p in human colorectal cancer, induces apoptosis and inhibits cell proliferation. *Cancer Gene Ther*. 2016;23:199-205. https://doi.org/10.1038/cgt.2016.10
13. Jiang W, Xu X, Deng S, et al. Methylation of kruppel-like factor 2 (KLF2) associates with its expression and non-small cell lung cancer progression. *Am J Transl Res*. 2017;9:2024-2037.
14. Jha P, Das H. KLF2 in regulation of NF-kappaB-mediated immune cell function and inflammation. *Int J Mol Sci*. 2017;18:pii:E2383. https://doi.org/10.3390/ijms18112383
15. Lv J, Gu WL, Chen CX. Effect of gentiopicroside on experimental acute pancreatitis induced by retrograde injection of sodium taurocholate into the biliopancreatic duct in rats. *Fitoterapia*. 2015;102:127-133. https://doi.org/10.1016/j.fitote.2015.03.002
16. Jiang CY, Wang W. Resistin aggravates the expression of proinflammatory cytokines in ceruleinstimulated AR42J pancreatic acinar cells. *Mol Med Rep*. 2017;15:502-506. https://doi.org/10.3892/mmr.2016.6027
17. Livak KJ, Schmittgen TD. Analysis of relative gene expression data using real-time quantitative PCR and the 2(-Delta Delta C (T)) method. *Methods*. 2001;25:402-408. https://doi.org/10.1006/meth.2001.1262
18. Jeon TJ, Park JY. Clinical significance of the neutrophil-lymphocyte ratio as an early predictive marker for adverse outcomes in patients with acute pancreatitis. *World J Gastroenterol*. 2017;23:3883-3889. https://doi.org/10.3748/wjg.v23.i21.3883
19. Lugea A, Waldron RT, Mareninova OA, et al. Human pancreatic acinar cells: proteomic characterization, physiologic

responses, and organellar disorders in ex vivo pancreatitis. *Am J Pathol*. 2017;187:2726-2743. https://doi.org/10.1016/j.ajpath.2017.08.017

20. Forsmark CE, Vege SS, Wilcox CM. Acute pancreatitis. *N Engl J Med*. 2016;375:1972-1981. https://doi.org/10.1056/NEJMra1505202
21. Yue J, Wan F, Zhang Q, et al. Effect of glucocorticoids on miRNA expression spectrum of rat femoral head microcirculation endothelial cells. *Gene*. 2018;651:126-133. https://doi.org/10.1016/j.gene.2018.01.057
22. Fu F, Jiang W, Zhou L, Chen Z. Circulating exosomal miR-17-5p and miR-92a-3p predict pathologic stage and grade of colorectal cancer. *Transl Oncol*. 2018;11:221-232. https://doi.org/10.1016/j.tranon.2017.12.012
23. Wang Q, Teng Y, Wang R, et al. The long non-coding RNA SNHG14 inhibits cell proliferation and invasion and promotes apoptosis by sponging miR-92a-3p in glioma. *Oncotarget*. 2018;9:12112-12124. https://doi.org/10.18632/oncotarget.23960
24. Zhu S, Zhang L, Zhao Z, et al. MicroRNA92a3p inhibits the cell proliferation, migration and invasion of Wilms tumor by targeting NOTCH1. *Oncol Rep*. 2018;40:571-578. https://doi.org/10.3892/or.2018.6458
25. Casadei L, Calore F, Creighton CJ, et al. Exosome-derived miR-25-3p and miR-92a-3p stimulate liposarcoma progression. *Cancer Res*. 2017;77:3846-3856. https://doi.org/10.1158/0008-5472.CAN-16-2984
26. Shi J, Zhou LR, Wang XS, et al. KLF2 attenuates bleomycin-induced pulmonary fibrosis and inflammation with regulation of AP-1. *Biochem Biophys Res Commun*. 2018;495:20-26. https://doi.org/10.1016/j.bbrc.2017.10.114
27. Zhang D, Dai Y, Cai Y, et al. KLF2 is downregulated in pancreatic ductal adenocarcinoma and inhibits the growth and migration of cancer cells. *Tumour Biol*. 2016a;37:3425-3431. https://doi.org/10.1007/s13277-015-4053-3
28. Zou K, Lu X, Ye K, Wang C, You T, Chen J. Kruppel-like factor 2 promotes cell proliferation in hepatocellular carcinoma through up-regulation of c-myc. *Cancer Biol Ther*. 2016;17:20-26. https://doi.org/10.1080/15384047.2015.1108484
29. Qian D, Wei G, Xu C, et al. Bone marrow-derived mesenchymal stem cells (BMSCs) repair acute necrotized pancreatitis by secreting microRNA-9 to target the NF-kappaB1/p50 gene in rats. *Sci Rep*. 2017;7:581. https://doi.org/10.1038/s41598-017-00629-3
30. Zhang J, Xu R, Tao X, et al. TAT-IL-24-KDEL-induced apoptosis is inhibited by survivin but restored by the small molecular survivin inhibitor, YM155, in cancer cells. *Oncotarget*. 2016b;7:37030-37042. https://doi.org/10.18632/oncotarget.9458

How to cite this article: Ling L, Wang H-F, Li J, Li Y, Gu C-D. Downregulated microRNA-92a-3p inhibits apoptosis and promotes proliferation of pancreatic acinar cells in acute pancreatitis by enhancing KLF2 expression. *J Cell Biochem*. 2020;121:3739–3751. https://doi.org/10.1002/jcb.29517